2018 IEEE International Conference on Robotics and Automation (ICRA)
May 21-25, 2018, Brisbane, Australia

Clothoid-Based Global Path Planning for Autonomous Vehicles in Urban Scenarios

Júnior A. R. Silva[1] and Valdir Grassi Jr.[1]

Abstract— **Intelligent vehicles require an efficient way to compute a feasible path that connects its current localization to a destination point. To achieve that, the knowledge about the road network, including its geometry, is important since connections between roads can be used in the path planning. This work consists on computing a feasible global path for autonomous vehicles with kinematic constraints. Piecewise linear continuous-curvature paths composed of clothoids, circular arcs, and straight lines are used for this purpose. Low curvature derivatives provide comfort to passengers. This approach provides a compact road network representation as only the parameters of the curves are stored. A real urban scenario with straight and curved roads, multiple lanes, intersections, and roundabouts is modeled and the proposed approach is validated. As a result of the proposed approaches, door-to-door global continuous-curvature paths are generated considering the shortest traveled distance.**

I. INTRODUCTION

Autonomous vehicles are a promising evolution in the nowadays transportation of people and goods. They can provide a better use of the travel time, reduction in pollutants emission and in crashes caused by human mistakes, improvements in the traffic flow, etc. [1]. In door-to-door assistance applications, those vehicles must be able to autonomously define a route from its current position to an addressed destination.

At the highest level in the decision-making hierarchy, the vehicle must find a route taking into account connections between the roads that compose the structured environment the vehicle is inserted in, the so-called road network [2], which has been a matter of research in ADAS (Advanced Driver-Assistance Systems) [3][4] and in path planning for autonomous vehicles [5]. In addition to the structure representation, it is desirable that the road network model have an accurate road geometry representation [4], which may be used to assist the vehicle in the global path computation [6]. Moreover, the path tracking controller can benefit from accurate and smooth reference paths [7]. In addition, the road network model must have a compact format in order to avoid large amount of storage data [8].

Interpolating curves such as cubic splines, B-splines, Bézier and clothoid curves are commonly applied to the road shape modeling, since they are smooth and can be parameterized by control points [9], thus reducing the amount of data storage. Generally interpolating curves are used to model a stretch of road [10][11] or closed-circuits [8]. However, a path planning approach considering a structured environment with many roadway segments are not discussed. This is addressed in [6], where straight single-lane roads separated by either intersections or roundabouts are automatically connected using Bézier curves. Nevertheless, a more complex urban scenario that contains curved lanes and double-lane roads were not presented.

This paper proposes a clothoid-based road network model for autonomous vehicles, applied to path planning in urban scenarios with curved lanes, double-lane roads, intersections and roundabouts. Clothoids control points are used to accurately describe the geometry of road lanes, and are posteriorly used in on-line interpolation, resulting in a kinematic feasible path with a bounded piecewise linear continuous curvature and low curvature rate change. Another contribution of this paper is the clothoid-based lane change path planner for non-parallel configuration change with prescribed longitudinal traveled distance with low curvature derivative. This work can be seen as a continuity of the author's previous paper [12], where a parametric-based roundabout planner using clothoids were presented.

As the quality of curvature is a concern in path planning for autonomous vehicle, the resulting road network model must provide a framework that allows path computation as in conformity with vehicle's physical limits. The use of clothoids in this work is justified because the control over the curvature can be obtained in a direct manner, since clothoids are parametric curves whose curvature varies linearly with respect to its arc length. This fact makes them largely used in road shape design [13], as the curvature rate change can be controlled in order to provide comfort to passengers. This can not be intuitively obtained by Polynomial curves (cubic splines, B-splines, Bézier). In some cases it is even impossible to achieve the desired curvature profile using such curves [14].

The remaining of this paper is organized as follows: the vehicle's kinematic model is described in Section II; Section III presents the road network model construction, detailing how the lanes and roundabouts can be parameterized in order to represent the physical elements on a real map; Section IV depicted the best route computation regarding the traveled distance and the path planning of intersections and lane changes; Section V shows the experimental results of the clothoid-based road network considering a real map,

*This work was supported by the Coordination for the Improvement of Higher Education Personnel (CAPES) under grants 1584685, the National Institute of Science and Technology (INCT) under grant 465755/2014-3 of the Brazilian National Research Council (CNPq), and grant 2014/50851-0 of the São Paulo Research Foundation (FAPESP).

[1]The authors are with the Department of Electrical and Computer Engineering, São Carlos School of Engineering, University of São Paulo, São Carlos, Brazil junior.anderson@usp.br, vgrassi@usp.br.

the data storage reduction and the continuous-curvature path computation between two assigned points on the map; finally, remarks and future work are presented in Section VI.

II. KINEMATIC MODEL OF THE CAR LIKE-VEHICLE

The constructive aspects of the vehicle are relevant and must be considered in order to know whether it is able to track the planned path. Fig. 1 shows a bicycle model used to represent car-like vehicles, which are characterized by Ackerman steering geometry [15], moving with longitudinal velocity v. The front wheel is able to turn and gives the steering angle ϕ, whereas the rear wheel is always aligned with the bicycle body. In Fig. 1 it should be noted that θ gives the heading of the vehicle and P is the guide point, which is controlled in order to follow the assigned path. The intersection between the lines that pass through the rear and front wheels axes gives the Instantaneous Center of Curvature (ICC). The distance between the ICC and P represents the radius of curvature R. The curvature of the vehicle is given by $\kappa = 1/R$.

Considering that the wheels roll without slipping and the vehicle is traveling at low speeds ($v < 15$m/s) only the kinematic equations can be considered, since the lateral dynamic effects can be neglected [7]. Hence, the considerations made so far result in the following kinematic model [16]

$$\begin{bmatrix} \dot{x} \\ \dot{y} \\ \dot{\theta} \\ \dot{\kappa} \end{bmatrix} = \begin{bmatrix} \cos\theta \\ \sin\theta \\ \kappa \\ 0 \end{bmatrix} v + \begin{bmatrix} 0 \\ 0 \\ 0 \\ 1 \end{bmatrix} \tau, \tag{1}$$

where $\tau = \dot{\phi}/(D_{bl}\cos^2\phi)$.

In (1), four different states are defined: x and y coordinates on the plane; the heading θ; and the curvature κ. This set of states represents the pose or configuration q of the vehicle. The configuration space represents the different configurations the vehicle can assume. Since the vehicle can only perform curves with a bounded curvature regarding its constructive aspects, $|\kappa| < \kappa_{max}$, the maximum absolute curvature allowed. Also, the steering angle can not instantaneously change, requiring that $|\dot{\kappa}| < \dot{\kappa}_{max}$, the maximum absolute curvature rate change that the vehicle can perform. Hence, it is important to know the curvature along the path length to be tracked by the vehicle. It makes

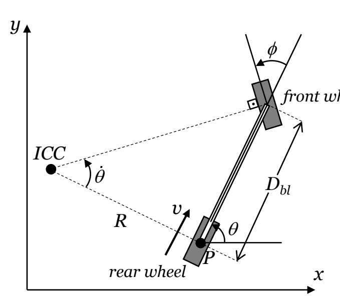

Fig. 1: Geometry of a bicycle model. The ICC is determined from the length of the bicycle body D_{bl} and the steering angle ϕ.

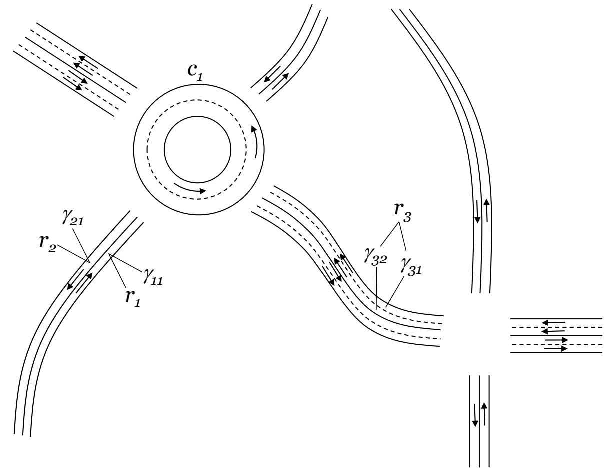

Fig. 2: Representative example of a road network representation. Roads are separated by solid lines, where dashed lines separate lanes.

the representation of the path in space-domain more suitable. Making $v(t)dt = ds$ and assuming $v(t) \neq 0$ as a continuous function, from (1):

$$\begin{aligned} dx(s)/ds &= \cos(\theta(s)) \\ dy(s)/ds &= \sin(\theta(s)) \\ d\theta(s)/ds &= \kappa(s) \\ d\kappa(s)/ds &= \sigma(s), \end{aligned} \tag{2}$$

where s is the traveled distance along the path and $\sigma(s)$ is the variation of the curvature with respect to s.

III. ROAD NETWORK MODEL

A representative example of a road network is depicted in Fig. 2. Three elements are considered in the topological representation:

- **Lanes**: are strips in the roads which can accommodate a single line of vehicles.
- **Intersections**: are junctions where two or more lanes meet or cross.
- **Roundabouts**: like intersections, are used to join lanes and are characterized by a circular roadway that enforces speed reduction.

In this paper, a clothoid-based model used to calculate piecewise linear continuous-curvature curves is proposed, in such a way to guarantee curvature continuity along the whole planned route with bounded curvature and low curvature rate change. The physical road network **Z** is given by **Z = (C, R)**, where **C** is the set of roundabouts $\{\mathbf{c}_i\}_{i=1}^{N_c}$, and **R** is the set of roads $\{\mathbf{r}_i\}_{i=1}^{N_r}$. The roundabout **c** is defined by its center C_{rbt} and radii $\{r_{rbt}\}_{i=1}^{N_{r_{rbt}}}$, **c** = ($C_{rbt}$, $\{r_{rbt}\}_{i=1}^{N_{r_{rbt}}}$), which means that multiple lanes are allowed in the same roundabout. The road **r** is the set of lanes belonging to same carriageway **r = (T,** u**)**, where **T** is the set of lanes $\{\gamma_i\}_{i=1}^{N_\gamma}$ and u indicates which roundabout the road ends at. When the road ends at an intersection, u is set as 0. The lane γ is defined as $\gamma = (\mathbf{S}_\gamma, n, \lambda_i, \lambda_o, r_{off_i}, r_{off_o}, \boldsymbol{q}_s, \boldsymbol{q}_e)$, where $\mathbf{S}_\gamma$ is the set of parameters describing all clothoids that compose the lane (Section III-A), n is the relative position of the lane inside the road (the number 1 is assigned to leftmost lanes by convention [3]), and λ_i, λ_o, rd_{off_i} and rd_{off_o} are parameters used in the roundabout path planning (Section III-B). $\boldsymbol{q}_s$ and $\boldsymbol{q}_e$ are the path configurations at the start and end of the lane, respectively.

It is considered that roads can be connected by roundabouts and intersections. In order to compute a route between start and destination points, a connection matrix $A_{m\times m}$ is defined, where m is the number of roundabouts and intersections on the map. Each road must end either at a roundabout or at an intersection, which are considered as connection entities.

A. Clothoid-based lane geometry parametrization

A road shape parametrization can significantly reduce the amount of stored data, if compared to a road representation composed by a set of waypoints collected by GPS. Hence, clothoids can be satisfactorily used to represent the road geometry, since they are smooth curves and can be parameterized by its curvature. The Cartesian coordinates of clothoids are defined in the form of the Fresnal's integrals as

$$x(\xi) = \pi B \cdot C(\xi) \tag{3a}$$

$$y(\xi) = \pi B \cdot S(\xi), \tag{3b}$$

where ξ is the arc-length parameter, $B = 1/\sqrt{\pi\sigma}$ is the scaling factor, σ is constant because of the curvature linearity and

$$C(\xi) = \int_0^{\xi} \cos\left(\frac{\pi}{2}\zeta^2\right) d\zeta \tag{3c}$$

$$S(\xi) = \int_0^{\xi} \sin\left(\frac{\pi}{2}\zeta^2\right) d\zeta \tag{3d}$$

are the Fresnel's integrals [17]. The curvature is given by $\kappa(\xi) = \xi/B$, and the traveled distance s along the clothoid is found making $s = \xi/(\sigma B)$.

The algorithm presented in [7] is used here to make the piecewise linearization of the curvature by an optimization technique. The function to be minimized and the inequality constraints are

$$\begin{aligned} \min_{\kappa} \quad & ||W \odot D\kappa||_1 \\ \text{s. t.} \quad & |x(\kappa) - x_{raw}| \le \varepsilon \\ & |y(\kappa) - y_{raw}| \le \varepsilon, \end{aligned} \tag{4}$$

where x and y are the coordinate vectors of all points of the reconstructed curve and κ is the curvature vector. x_{raw} and y_{raw} are the coordinate vectors of all points of the original curve, D is the second order difference operator matrix, ε is the bounded error vector, $\odot$ is the Hadamard product and W is the vector that contains weights that are initially set to 1 and updated at each iteration as

$$W_{j+1} = \frac{1}{W_j \odot D\kappa}, \tag{5}$$

performing a normalization so that the weights sum up to the number of samples. Thereby, the values of $D\kappa$ that are close to zero receive higher weights enforcing the second difference of the curvature to be zero in many points, performing a ℓ_0-norm computation. A new clothoid starts at those points where $D\kappa \neq 0$.

As it is discussed later, the roundabout and intersection paths always have null curvature at the start and end configurations. Hence, in this paper, the minimization problem given in [7] is modified in order to make the curvature at the start and end of all lanes equal to 0 to achieve curvature continuity. Therefore, two constraints are added to the minimization problem and (4) becomes

$$\begin{aligned} \min_{\kappa} \quad & ||W \odot D\kappa||_1 \\ \text{s. t.} \quad & |x(\kappa) - x_{raw}| \le \varepsilon \\ & |y(\kappa) - y_{raw}| \le \varepsilon \\ & \kappa_s = 0 \\ & \kappa_e = 0, \end{aligned} \tag{6}$$

where κ_s and κ_e are the start and end curvatures, respectively.

After the optimization, $\kappa(s)$ is a piecewise linear function. The information about σ and s of all clothoids are stored in the form

$$\mathbf{S}_\gamma = \begin{bmatrix} \sigma_1 & \sigma_2 & \dots & \sigma_k \\ s_1 & s_2 & \dots & s_k \end{bmatrix}^T, \tag{7}$$

where k is the number of clothoids in the lane.

In this way, once the start configuration $\boldsymbol{q}_s = [x_s \quad y_s \quad \theta_s \quad 0]^T$ is known, the lane path can be computed. When the start curvature, and curvature derivative of any curve segment is not null, the computation is performed using (3). Otherwise, the curve segment is either a circular arc or a straight line, making the computation straightforward. Also, the end configuration $\boldsymbol{q}_e = [x_e \quad y_e \quad \theta_e \quad 0]^T$ is required in order to allow the computation of connection paths between lanes, i. e. intersections and roundabouts.

B. Roundabout parameters

The parametric-based roundabout path planing approach used here to compute smooth paths with bounded curvature was developed in an author's previous work [12]. The planned path connects the configurations at the roundabout entrance $\boldsymbol{q}_s$ and exit $\boldsymbol{q}_g$, using piecewise linear continuous-curvature curves.

Fig. 3 shows the scheme used to compute such paths, where $C_{rbt} = [x_{C_{rbt}} \quad y_{C_{rbt}}]^T$ and r_{rbt} are the roundabout center and radius, respectively. $\boldsymbol{q}_i$ is the configuration just before entering the circulatory roadway and it is determined from the entrance angle λ_i and the offset radius r_{off_i}. The same follows for $\boldsymbol{q}_o$, the configuration just after leaving the circulatory roadway. However, λ_o and r_{off_o} are used instead.

The desired path is automatically computed once C_{rbt}, r_{rbt}, $\boldsymbol{q}_s$, $\boldsymbol{q}_g$, λ_i, r_{off_i}, λ_o and r_{off_o} are given. λ and r_{off} depends on the geometry of the roundabout entrance and exit and are adjusted in order to fit the lanes. The required parameters are determined off-line, but the path computation is performed

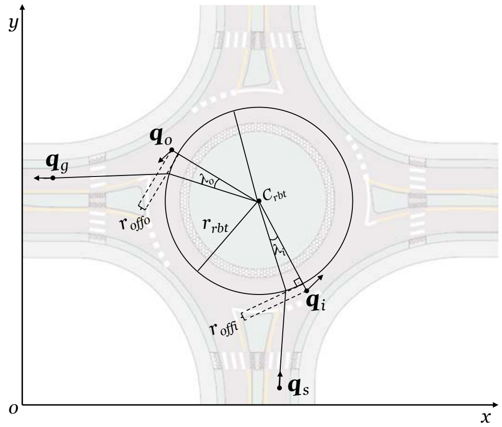

Fig. 3: Scheme depicting the roundabout path planning approach (adapted from [12]).

on-line. When the connection between two lanes is not a roundabout, λ_i, r_{off_i}, λ_o and r_{off_o} are set to 0. For this situation, the connection path is an intersection, which not requires extra parameters to be computed (Section IV-B).

IV. GLOBAL PATH PLANNING

The route is determined between a start point P_s and a goal point P_g on the map. The first task is to determine which lanes these points belong to. This is done simply by considering the distance between the assigned points to all lanes on the map. The closest lane to P_s is chosen as the start lane. The same follows for P_g.

After that, the points must be localized inside the lanes. Fig. 4 depicts that P_s and P_g are localized with respect to s inside the initial and destination lane, respectively. The planned path starts at s_s and ends s_e, considering the start and destination lane, respectively (see Fig. 4).

A. Best route computation

It is possible to compute a route from P_s to P_g using A and considering each intersection and roundabout as a node inside a directed graph, as in Fig. 5. The edges in the graph are roads with an associated cost. In this work, the cost is related to the total length of each road. In order to compute a route, two nodes representing the current vehicle position and the target point are added to the graph according to the roads they belong, and the costs are modified according to the position of P_s and P_g. The best route can be computed by searching the nodes connecting P_s and P_g that yields the shortest path. The well-known Dijkstra's algorithm [18] is applied here for this purpose.

B. Intersection path

The computation of paths with a minimal amount of steering is performed according to [19]. The clothoid length L is calculated from the clothoid deflection δ (Fig. 6) as

$$L = \frac{y_{ct}}{\sin_c \delta} = \frac{x_{ct}}{\cos_c \delta}, \quad \kappa = \frac{2\delta}{L}, \quad \sigma = \frac{\kappa}{L}, \tag{8}$$

where x_{ct} is the clothoid forward traveled distance, y_{ct} is the clothoid lateral traveled distance and

$$\sin_c \delta = \begin{cases} (-\sin\delta \cdot C(\eta) + \cos\delta \cdot S(\eta))/\eta, & \delta > 0 \\ 0, & \delta = 0 \\ -\sin_c(-\delta), & \delta < 0 \end{cases}$$
$$\cos_c \delta = \begin{cases} (\cos\delta \cdot C(\eta) + \sin\delta \cdot S(\eta))/\eta, & \delta > 0 \\ 1, & \delta = 0 \\ \cos_c(-\delta), & \delta < 0 \end{cases} \tag{9}$$

where C and S are the Fresnel's integrals and $\eta = \sqrt{2|\delta|/\pi}$.

Right and left turn curves can be achieved by connecting two opposite clothoids, in order to provide null curvature at the start and end configuration of the path, where 2δ is the total defection of the turn.

C. Lane change path

The vehicle might perform lane changes in order to reach its destination. In this paper, it is assumed that lane changes are required in the following scenarios:

- The vehicle must be on the rightmost lane when performing right turns at intersections and when taking the first and second exits at roundabouts.
- The vehicle must be on the leftmost lane when performing left turns at intersections and when when taking the third and fourth exits at roundabouts.

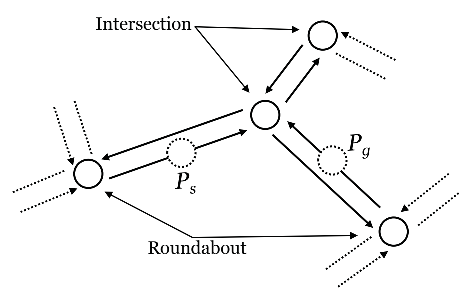

Fig. 5: Example of a graph representing connections between intersections and roundabouts.

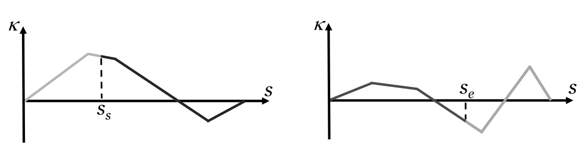

(a) Initial lane. The planned path starts at s_s.

(b) Destination lane. The planned path ends at s_e.

Fig. 4: Curvature profiles of initial and destination lanes.

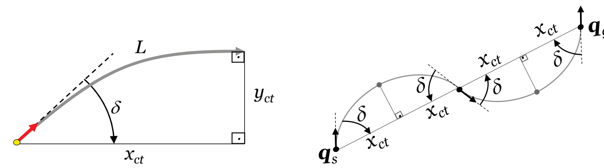

(a) Clothoid segment (adapted from [19]).

(b) Interpolation using four symmetrical clothoids segments.

Fig. 6: Clothoid trigonometry applied to path generation.

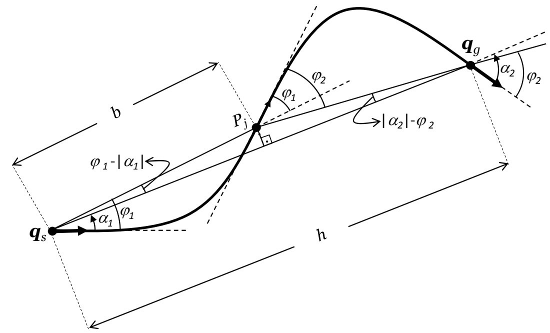

Fig. 7: Scheme depicting the computation of the lane change parameters.

Wilde [19] showed how to connect clothoids to construct lane change maneuvers, as in Fig. 6b, with curvature continuity between the start configuration $\boldsymbol{q}_s = [x_s \quad y_s \quad \theta_s \quad \kappa_s]^T$ and the goal configuration $\boldsymbol{q}_g = [x_g \quad y_g \quad \theta_g \quad \kappa_g]^T$, where $\kappa_s = \kappa_g = 0$. However, this approach is constrained to parallel configuration changes, since four symmetrical clothoids are required. Scheuer and Fraichard [20] showed how two opposite curves, each composed by two symmetric clothoids, can be used to computed non-parallel configuration change paths with minimal length. These paths may, nevertheless, be jerky because the short traveled distance in order to perform the change configuration. In this paper, lane change maneuvers are extended to the case where $\theta_s \neq \theta_g$, according to Fig. 7, where P_j is the join point connecting the two opposite turns and $\theta_s = 0$ without lost of generality. The two turns have a minimal amount of steering, as it is presented in Section IV-B, which means symmetrical configuration changes at each turn. For simplicity, P_j is assumed to lie on a vertex of an isosceles triangle, where $\boldsymbol{q}_s$ and $\boldsymbol{q}_g$ are the other vertexes. In order to accomplish the imposed requirements, the following linear system must be satisfied:

$$\begin{cases} 2\varphi_1 - 2\varphi_2 - |\alpha_1| + |\alpha_2| = 0 \\ \varphi_1 - |\alpha_1| = |\alpha_2| - \varphi_2, \end{cases} \tag{10}$$

where φ_1, φ_2, α_1 and α_2 are angles defined according to Fig. 7. b is the distance from $\boldsymbol{q}_s$ to P_j and h is the distance form $\boldsymbol{q}_g$ to $\boldsymbol{q}_g$. The first equation is the sum of the interior angles of a triangle, which must be equal to π rad. The second one is the restriction to construct an isosceles triangle. Solving (10) yields

$$\varphi_1 = \frac{3|\alpha_1| + |\alpha_2|}{4}, \quad \varphi_2 = \frac{|\alpha_2| - |\alpha_1| + 2\varphi_1}{2}. \tag{11}$$

From the law of cosine it is possible to get the following system:

$$\begin{cases} b^2 = h^2 + b^2 - 2bh \cdot \cos(\varphi_1 - |\alpha_1|) \\ b^2 = h^2 + b^2 - 2bh \cdot \cos(|\alpha_2| - \varphi_2) \end{cases} \tag{12}$$

which yields

$$b = \frac{h}{\cos(\varphi_1 - |\alpha_1|) \cdot \cos(|\alpha_2| - \varphi_2)}. \tag{13}$$

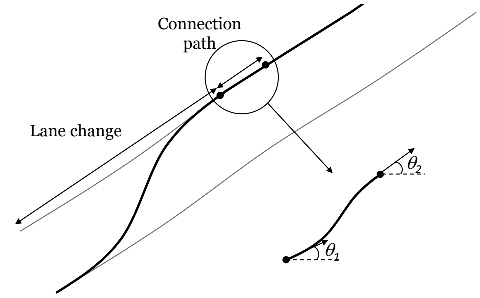

(a) Path.

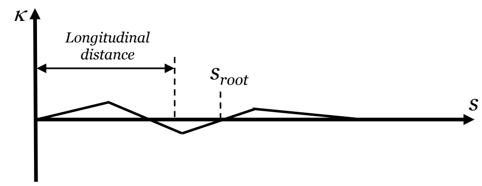

(b) Departure lane curvature.

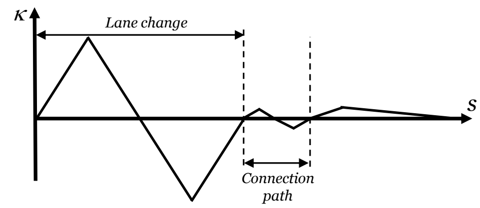

(c) Final curvature after the lane change.

Fig. 8: Scheme depicting the lane change path planning.

φ_1 and b are used to determine P_j in such a way that $x_{ct} = b/2$, the total deflection angles are $2\varphi_1$ and $2\varphi_2$ for the left and right turns, respectively. Now, (9) and (8) can be used to compute the parameters of the curve segments in the path.

The scheme depicting the lane change maneuver is shown in Fig. 8. The approach used to compute lane change paths is constrained to have null curvature at the start and end points. A good choice to initiate the lane change maneuver is at the start point of the departure lane, since the curvature is null at that point, according to (6). The whole maneuver could be concluded using only one non-parallel configuration change, but in this way the longitudinal traveled distance would be constraint to the location of the next point of null curvature on the destination lane, s_{root} (Fig. 8b), since continuous curvature is pursued. Therefore, the maneuver is divided into two steps: firstly, a lane change with an assigned longitudinal distance distance is computed. Finally, it is connected to the destination by another non-parallel configuration change path. Fig. 8c depicts the final profile of curvature after performing the lane change.

V. EXPERIMENTAL RESULTS

A probe-vehicle equipped with a GPS-RTK with a 4 cm maximum deviation and a 10 Hz sampling rate was used to acquire data information at USP - São Carlos, Campus 2, as the driver tried to keep the vehicle in the lane center. Since straight and curved lanes, roundabouts, and double-lane roads are present, most of the attributes of the global

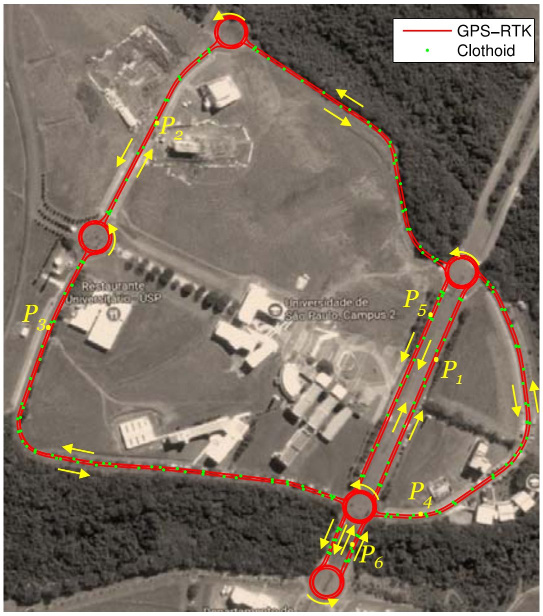

Fig. 9: A road network considering a real map. The solid lines represent the center of the lanes. Two adjacent green dots define a clothoid segment.

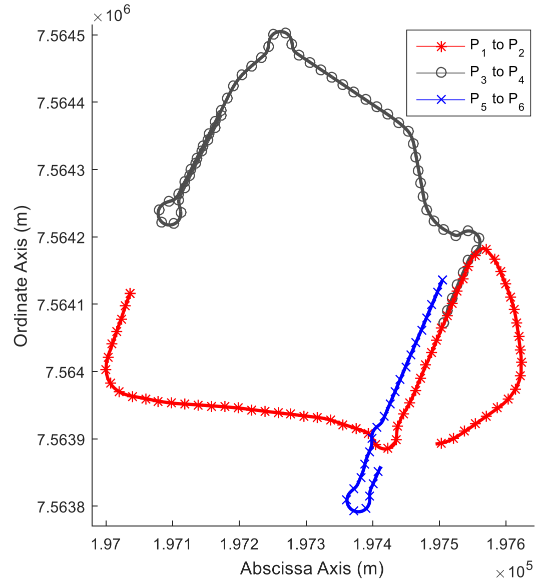

Fig. 10: Planned paths considering points P_i in Fig. 9.

planner can be verified. The resulting map can be seen in Fig. 9.

The beginning and end of each lane were manually defined based on the positions of roundabouts and intersections. The resulting road network model is composed by 12 roads, 16 lanes, and 5 roundabouts, where 4 roads are double-lane. A total of 13582 GPS points were acquired in the mapping process, so summing up to 27164 point coordinates. After the parametrization of lanes and roundabouts the amount of data was reduced to 586 values, where:

- **Lane geometry** S_γ: 173 clothoids were required to represent all lanes with a 0.1 m tolerance, summing up to 346 values (σ and s).
- $\boldsymbol{q}_s$ and $\boldsymbol{q}_e$: The start and end configurations of each lane require a total of 8 parameters to be stored, since each configuration has four states. Since there are 16 lanes, the total of values sums up to 128.
- u: 12 values (one for each road).
- n: 16 values (one for each lane).
- λ_i, λ_o, r_{off_i} and r_{off_o}: 4 values for each lane, summing up to 64 values.
- **Roundabout parameters**: 5 roundabout centers, summing up to 10 values (x and y coordinates), and 10 roundabout radii, since all roundabouts are double-lane.

In this way, there is a reduction of 46.3 times in the storage data. Despite that, the path can be computed in such a way to ensure smoothness, continuous curvature and low curvature rate, as it can be verified in Fig. 10 and 11. Three different routes are considered in the path planning: P_1 to P_2, P_3 to P_4 and P_5 to P_6. A 0.2 m^{-1} maximum absolute curvature for the vehicle for the roundabout path planning [12] is considered and the lane changes are performed considering a 30 m longitudinal distance.

In the first path, P_1 to P_2, a lane change, starting at P_1 is required since the start lane is the rightmost one on the road and the third exit is taken at the roundabout. This should be noted in Fig. 11a. Three roundabout are taken until P_2 is reached. The maximum curvature is reached in the second path (P_3 to P_4), as it can be seen in Fig. 11a and the path travels along two roundabouts. When going from P_5 to P_6, a lane change is performed after the first roundabout has been taken.

The road network and the path planning approach were implemented using *Python* language in a common personal computer (Intel Core I7 3770 3.4GHz). The Fresnal's integrals were computed using the real-time approximation of clothoids described in [21], where a 10^{-4} m approximation error was considered (in the worst case), since Fresnel's integrals have no analytical solution [9]. After running the algorithm numerous times considering different routes, the maximum time taken in the total planning was 1.43 seconds for a 0.1 m step, i.e. the distance between two adjacent coordinate points, and 0.74 seconds for a 0.5 m step. The results can be considered good, since the route planning is made before the vehicle initiates the travel ($v = 0$), characterizing a non-risky situation.

The curvature profile depicted in Fig. 11a is bounded to the assigned maximum value that the vehicle can drive. The low rate curvature change is associated with passenger's comfort. Since there is no abrupt change in the curvature, it is expected that the vehicle steering angle will smoothly vary during the path tracking.

VI. CONCLUSIONS

The proposed road network model was able to satisfactorily represent a real map, considering an urban scenario. Curvature continuity was guaranteed even at the connections between lanes. The time taken in the path computation can

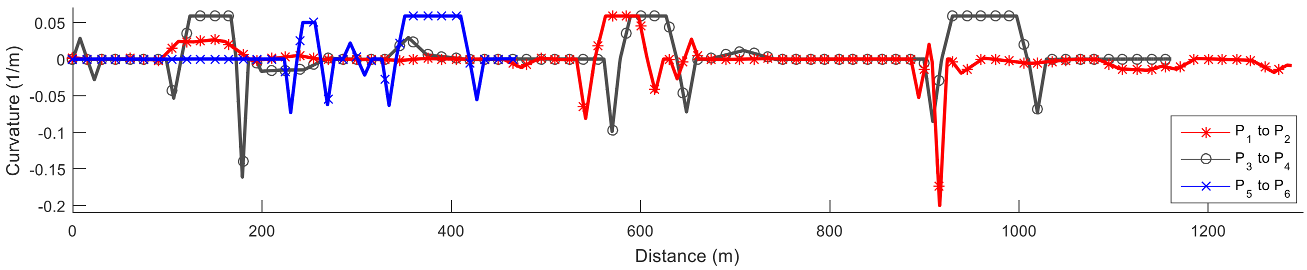

(a) Curvature

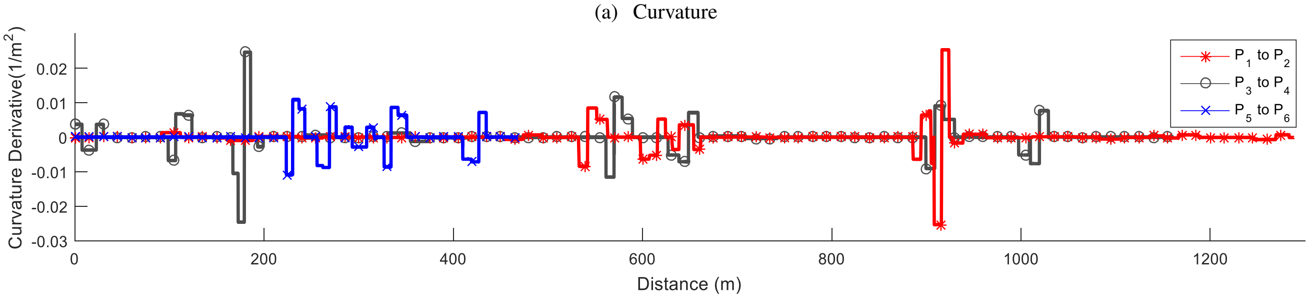

(b) Curvature derivative

Fig. 11: Curvature, and curvature derivative of the paths depicted in Fig. 10.

be considered good, since the route is computed before the vehicle starts the travel.

For future work, an automatic road network construction might be addressed in order to reduce the time expended in this task. Also, a local path planning, like obstacle avoidance, has to be considered. In this way, lane changes may have to be executed in arbitrary positions inside the lane and an approach to maintain the overall curvature continuity, even in this situation, must be developed.

ACKNOWLEDGMENT

The authors would like to thank CAPES, INCT, CNPq and FAPESP for supporting the work described in this paper, the Laboratory of Intelligent Systems (LASI) and the Laboratory of Mobile Robotics (LRM) at the University of São Paulo.

REFERENCES

[1] C. Katrakazas, M. Quddus, W.-H. Chen, and L. Deka, "Real-time motion planning methods for autonomous on-road driving: State-of-the-art and future research directions," *Transportation Research Part C: Emerging Technologies*, vol. 60, pp. 416–442, 2015.

[2] B. Paden, M. Čáp, S. Z. Yong, D. Yershov, and E. Frazzoli, "A survey of motion planning and control techniques for self-driving urban vehicles," *IEEE Transactions on Intelligent Vehicles*, vol. 1, no. 1, pp. 33–55, 2016.

[3] D. Bétaille and R. Toledo-Moreo, "Creating enhanced maps for lane-level vehicle navigation," *IEEE Transactions on Intelligent Transportation Systems*, vol. 11, no. 4, pp. 786–798, 2010.

[4] T. Zhang, S. Arrigoni, M. Garozzo, D.-g. Yang, and F. Cheli, "A lane-level road network model with global continuity," *Transportation Research Part C: Emerging Technologies*, vol. 71, pp. 32–50, 2016.

[5] M. Zoccoler, P. Y. Shinzato, A. Y. Hata, and D. F. Wolf, "Automatic semantic waypoint mapping applied to autonomous vehicles," in *Robotics*, pp. 96–113, Springer, 2014.

[6] J. P. Rastelli, R. Lattarulo, and F. Nashashibi, "Dynamic trajectory generation using continuous-curvature algorithms for door to door assistance vehicles," in *Intelligent Vehicles Symposium Proceedings, 2014 IEEE*, pp. 510–515, IEEE, 2014.

[7] P. F. Lima, M. Trincavelli, J. Mårtensson, and B. Wahlberg, "Clothoid-based model predictive control for autonomous driving," in *Control Conference (ECC), 2015 European*, pp. 2983–2990, IEEE, 2015.

[8] K. Jo and M. Sunwoo, "Generation of a precise roadway map for autonomous cars," *IEEE Transactions on Intelligent Transportation Systems*, vol. 15, no. 3, pp. 925–937, 2014.

[9] D. González, J. Pérez, V. Milanés, and F. Nashashibi, "A review of motion planning techniques for automated vehicles," *IEEE Transactions on Intelligent Transportation Systems*, vol. 17, no. 4, pp. 1135–1145, 2016.

[10] J. McCrae and K. Singh, "Sketching piecewise clothoid curves," *Computers & Graphics*, vol. 33, no. 4, pp. 452–461, 2009.

[11] K. Chu, M. Lee, and M. Sunwoo, "Local path planning for off-road autonomous driving with avoidance of static obstacles," *IEEE Transactions on Intelligent Transportation Systems*, vol. 13, no. 4, pp. 1599–1616, 2012.

[12] J. A. Silva and V. Grassi Jr., "Path planning at roundabouts using piecewise linear continuous curvature curves," in *Robotics Symposium (LARS) and 2017 Brazilian Symposium on Robotics (SBR), 2017 Latin American*, pp. 1–6, IEEE, 2017.

[13] A. Aashto, "Policy on geometric design of highways and streets," *American Association of State Highway and Transportation Officials, Washington, DC*, vol. 1, no. 990, p. 158, 2001.

[14] S. Havemann, J. Edelsbrunner, P. Wagner, and D. Fellner, "Curvature-controlled curve editing using piecewise clothoid curves," *Computers & Graphics*, vol. 37, no. 6, pp. 764–773, 2013.

[15] G. Dudek and M. Jenkin, *Computational Principles of Mobile Robotics*. New York, NY, USA: Cambridge University Press, 2nd ed., 2010.

[16] T. Fraichard and A. Scheuer, "From reeds and shepp's to continuous-curvature paths," *IEEE Transactions on Robotics*, vol. 20, no. 6, pp. 1025–1035, 2004.

[17] M. Abramowitz and I. A. Stegun, *Handbook of mathematical functions: with formulas, graphs, and mathematical tables*, vol. 55. Courier Corporation, 1964.

[18] E. W. Dijkstra, "A note on two problems in connexion with graphs," *Numerische mathematik*, vol. 1, no. 1, pp. 269–271, 1959.

[19] D. K. Wilde, "Computing clothoid segments for trajectory generation," in *2009 IEEE/RSJ International Conference on Intelligent Robots and Systems*, pp. 2440–2445, IEEE, 2009.

[20] A. Scheuer and T. Fraichard, "Planning continuous-curvature paths for car-like robots," in *Intelligent Robots and Systems' 96, IROS 96, Proceedings of the 1996 IEEE/RSJ International Conference on*, vol. 3, pp. 1304–1311, IEEE, 1996.

[21] M. Brezak and I. Petrovic, "Real-time approximation of clothoids with bounded error for path planning applications," *IEEE Transactions on Robotics*, vol. 30, no. 2, pp. 507–515, 2014.